IEEE Access
Multidisciplinary | Rapid Review | Open Access Journal

Received January 25, 2018, accepted March 4, 2018, date of publication March 12, 2018, date of current version April 18, 2018.

Digital Object Identifier 10.1109/ACCESS.2018.2814827

Neutrosophic Hough Transform-Based Track Initiation Method for Multiple Target Tracking

EN FAN[1,2], WEIXIN XIE[1], JIHONG PEI[1], (Member, IEEE), KELI HU[2], AND XIAOBIN LI[3]

[1]ATR National Key Laboratory of Defense Technology, Shenzhen University, Shenzhen 518060, China
[2]Department of Computer Science and Engineering, Shaoxing University, Shaoxing 312000, China
[3]Jožef Stefan International Postgraduate School, 1000 Ljubljana, Slovenia

Corresponding author: Jihong Pei (jhpei@szu.edu.cn)

This work was supported in part by the National Natural Science Foundation of China under Grant 61703280 and Grant 61603258, in part by the General Project of Educational Commission of Zhejiang Province under Grant 201635390, in part by the Plan Project of Science and Technology of Shaoxing City under Grant 2017B70056, in part by the Key Project of Science and Research of Shaoxing University under Grant 2015LG1006, and in part by the Public Welfare Technology Application Research-Industrial Project of Zhejiang Province under Grant 2016C31082.

ABSTRACT A neutrosophic Hough transform-based track initiation method (NHT-TI) is proposed to solve the uncertain track initiation problem in a complex surveillance environment. In the proposed method, a neutrosophic set is employed to describe the uncertain association of a measurement with different targets, which is divided into three categories, including the association with real targets, uncertain targets, and false targets, respectively. On this basis, the neutrosophic Hough transform (NHT) method is developed in the framework of the standard Hough transform (HT) method. Based on the sequential processing mode of the sensors, candidate temporary tracks are further defined to directly calculate the parameter points in the parameter space, which are utilized to calculate the contribution for the corresponding vote cells in the accumulation matrix by using the Gaussian membership function. Based on the scheme, the NHT method can avoid large traversal operations and reduce computation complexity of the HT method. Moreover, considering the effects of noises and clutters on track initiation, two constraint conditions related to the velocity information of moving targets and the time information of measurement sequences are introduced to suppress false tracks and reduce vote times. Finally, the real tracks can be determined by detecting the peaks of the global accumulation matrix. The performance of the proposed NHT-TI method is evaluated by using two experiments with simulated data and real data in two complex surveillance environments. The results are found to be better than those of the standard HT-based track initiation (HT-TI) method, the modified HT-TI method based on candidate temporary tracks and the improved HT-TI method in detection reliability and computational complexity.

INDEX TERMS Track initiation, Hough transform, neutrosophic set, data fusion, multiple target tracking.

I. INTRODUCTION

In military and civilian surveillance systems such as air traffic control (ATC), the real-time detection of moving targets in a surveillance field based on sensor measurements is a major challenge [1]. Track initiation is the primary problem in the process of multiple target tracking (MTT), which consists of track initiation, data association, filtering and termination [2]–[5]. Currently, track initiation methods can be divided into two main classes: i) sequential track initiation methods, such as the logic-based method [6] and the heuristic rule method [7], [8], which are generally applied in weakly cluttered environments, and ii) batch track initiation methods, such as the standard Hough transform-based track initiation (HT-TI) method and its modified versions [1], [9], [10], which are often employed in strongly cluttered environments. The purpose of this paper is to solve the uncertain track initiation problem in a strongly cluttered environment, and then the latter methods are mainly concerned. Although the batch track initiation methods can yield good performance through several scans in a highly cluttered environments, they are prone to increasing the computational burden and can even cause the explosive growth of association combinations [11]. Consequently, these methods are difficult to implement in real-time tracking systems. In addition, there is considerable uncertainty in the association between measurements and targets, particularly in complex situations in

which the tracks of targets are close or cross. Therefore, the implementation of track initiation has become increasingly difficult.

The Hough transform (HT) method was proposed by Hough [12] in 1962. It was first employed in the vote method to extract the straight-line features from images, and then it was further extended in track initiation applications by Smith [13]. Its major advantages include low sensitivity to local defect and strong robustness to random threshold detection. The HT method and its modified versions have been widely utilized in real applications [14]–[16]. Unfortunately, because of its high computational complexity mentioned above, the HT-TI method is slow and time-consuming. Thus, it is not appropriate for the use in a real-time surveillance system [1], [15]. Several studies have focused on solving this problem. Because the computational complexity of the HT-TI method mainly involves calculating the accumulation matrix, an effective solution is to modify the accumulation rule. Currently, most the modified HT methods employ the gradient magnitude accumulation rule, the probability accumulation rule, the kernel function accumulation rule, the binary accumulation rule, or the fuzzy accumulation rule [15]. However, these accumulation rules still need to calculate the contribution of each measurement for all the vote cells in the accumulation matrix. Therefore, the computational complexity cannot be significantly reduced.

As described above, many modified HT-TI methods have been developed. However, they mainly focused on the structural design of the track initiation process and have given little attention to the uncertain association between measurements and different targets in a complex surveillance environment, such as the presence of crossing targets, close targets and false targets. In these complex situations, the detection performance of the traditional track initiation methods may significantly decline. In addition, due to the effects of noises and clutters on track initiation, these methods are prone to generating false peaks and make the peaks of an accumulation matrix diverged and declined. The fuzzy HT (FHT) method in [17] uses the fuzzy membership function to replace the binary accumulation function, which is often applied in image detection [16], [18], [19]. Although the FHT method can somewhat overcome the decline of the peaks of the accumulation matrix, it cannot describe the uncertain association of a measurement with different targets in a complex environment. Hence, it is difficult to satisfy the practical requirements of real applications using this approach.

The neutrosophic set was proposed by Smarandache [20] in 1999 based on the intuitionistic fuzzy set and the fuzzy set. It has clear advantages in describing and processing the uncertain information [21], [22]. Consequently, the use of the neutrosophic set is a good strategy to describe the uncertain association in various applications such as image processing [23], video tracking [24], fault diagnosis [25] and natural language analysis [26]. In addition, incorporating the velocity information of moving targets and the time information of measurement sequences into the traditional track initiation methods can reduce false association and vote times [1], [6], [27]. Based on these factors, a neutrosophic Hough transform-based track initiation (NHT-TI) method is proposed to solve the uncertainty track initiation problem in complex tracking environments.

The major contributions are given as follows:

i) In a complex surveillance environment, the uncertain association of a measurement with targets in a complex tracking environment is first divided into three categories including the association with real targets, uncertain targets and false targets, respectively. On this basis, the uncertain association can be easily described by the neutrosophic set. Moreover, the NHT method is proposed for the uncertain track initiation in the framework of the HT. Because the NHT method employs the neutrosophic set to describe the uncertain association in complex track initiation, it can reduce false association combinations and improve correct detection rate.

ii) Based on the sequential processing mode of sensors, candidate temporary tracks are defined to calculate the parameter points, which correspond to the vote cells in the accumulation matrix. Consequently, only the corresponding vote cells in the accumulation matrix need to be counted. For this reason, the NHT can avoid large traversal operations in the HT method. Therefore, the computational complexity of the NHT method can be greatly reduced.

iii) In addition, considering the effects of noises and clutters on track initiation, two constraint conditions related to the velocity information of moving targets and the time information of measurement sequences are incorporated in the processing procedures of track initiation. Then, the NHT method can suppress false tracks and reduce vote times. Hence, the computational complexity of the NHT-TI method can be further reduced.

iv) Two complex initialized conditions with simulated data and real data are designed to illustrate the validity of the proposed NHT-TI method. The performance of the proposed method is compared with those of the standard HT-TI method, the modified HT-TI method and the improved HT-TI method. The results of the two experiments illustrate that the proposed NHT-TI method can realize track initiation effectively in a complex environment and achieve better performance for detecting straight-line tracks than those of other three track initiation methods.

The remainder of this paper is organized as follows. Section II provides a brief introduction of the basic neutrosophic set theory is given, and it is employed to describe the uncertain association of a measurement with different targets. Section III introduces the standard HT method and further develops the NHT method. In Section IV, the NHT-TI method is proposed. Section V presents the experimental results and the performance comparison with the standard HT-TI mothed, the modified HT-TI method based on

candidate temporary tracks (MHT-TI) and the improved HT-TI method (IHT-TI) [27]. Finally, the conclusions are provided in Section V.

II. ANALYSIS OF THE UNCERTAINTY OF TRACK INITIATION

To solve the uncertain track initiation problem in a complex environment, the uncertain association of a measurement with different targets is analyzed by using of the neutrosophic set theory. Moreover, the definitions of temporary tracks and candidate temporary tracks are introduced for convenient analysis.

A. BASIC THEORY OF THE NEUTROSOPHIC SET

The neutrosophic set usually considers each object E together with its opposite anti-E and with their spectrum of neutralities neut-E. Here, anti-E means neither E nor non-E, neut-E and anti-E together are also referred to as non-E. Neut-E depends on E, and anti-E may be indeterminate, neutral, unknown, contradictory, or imprecise [22]. The neutrosophic set can be measured by three components including the truth degree (T), the indeterminacy degree (I) and the falsity degree (F). These components are defined in a common observation space and are mutually independent. Therefore, the neutrosophic set can explicitly describe and measure the uncertainty of an object. It has an obvious advantage in describing and processing uncertain information compared with the intuitionistic fuzzy set and the fuzzy set.

The neutrosophic set and the single-valued neutrosophic set are defined as follows [20], [21], [25]:

Definition 1: Let U be a non-empty set; a neutrosophic set $\tilde{A}$ is defined in U and is expressed by

$$\tilde{A} = \left\{ < u, T_{\tilde{A}}(u), I_{\tilde{A}}(u), F_{\tilde{A}}(u) > | u \in U \right\} \tag{1}$$

where $T_{\tilde{A}}(u)$, $I_{\tilde{A}}(u)$ and $F_{\tilde{A}}(u)$ represent the truth-membership function, the indeterminacy-membership function, and the falsity-membership function of $\tilde{A}$, respectively. For $\forall u \in U$, they are standard or non-standard real subsets of $]^{-}0, 1^{+}[$ with potentially no connection between them, and the classical unit interval [0, 1] is used [20].

Definition 2: Let U be a non-empty set; a single-valued neutrosophic set $\tilde{A}$ is defined in U and is expressed by

$$\tilde{A} = \left\{ < u, T_{\tilde{A}}(u), I_{\tilde{A}}(u), F_{\tilde{A}}(u) > | u \in U \right\} \tag{2}$$

where $T_{\tilde{A}}(u)$, $I_{\tilde{A}}(u)$ and $F_{\tilde{A}}(u)$ represent the truth-membership function, the indeterminacy-membership function, and the falsity-membership function of $\tilde{A}$, respectively. For $\forall u \in U$, $T_{\tilde{A}}(u)$, $I_{\tilde{A}}(u)$, and $F_{\tilde{A}}(u) \in [0, 1]$.

B. DEFINING TEMPORARY TRACKS AND CANDIDATE TEMPORARY TRACKS

For convenience in the analysis, the definitions of temporary tracks and candidate temporary tracks are given in this subsection. In a real application, once a sensor receives a measurement, it must be immediately processed rather than at the end of the sampling period. Therefore, for simplicity in the following discussion, a temporary track $\boldsymbol{t}_{k,l}$ is defined as a set of two measurements $\boldsymbol{z}_{k-1,i}$ and $\boldsymbol{z}_{k,j}$ at two consecutive times from a common sensor:

$$\boldsymbol{t}_{k,l} = \{\boldsymbol{z}_{k-1,i}, \boldsymbol{z}_{k,j}\} \tag{3}$$

where $i = 1, 2, \cdots, n_{k-1}, j = 1, 2, \cdots, n_k$, and n_{k-1} and n_k are the numbers of measurements obtained by the sensor at $k-1$ and, respectively.

Due to the effect of clutters, one cannot directly confirm whether the temporary track is from a real target or if it possibly corresponds to a false track (alarm). Thus, a candidate temporary track $\boldsymbol{t}'_{k,l}$ is further defined as a set of any two measurements (including clutters) $\boldsymbol{z}_{k-1,i}$ and $\boldsymbol{z}_{k,j}$ at consecutive times from a common sensor:

$$\boldsymbol{t}'_{k,l} = \{\boldsymbol{z}_{k-1,i}, \boldsymbol{z}_{k,j}\} \tag{4}$$

where $i = 1, 2, \cdots, n_{k-1}, j = 1, 2, \cdots, n_k$, and n_{k-1} and n_k are the numbers of measurements obtained by the sensor at $k-1$ and k, respectively.

Therefore, a candidate temporary track might correspond to a real target or a false target. In addition, if a measurement simultaneously drops into the common tracking gate of two candidate temporary tracks (here corresponding to two real targets) in a complex situation as shown in Fig. 1, it could be from either of the two real targets or the uncertain target, which is defined in the next subsection. However, the association uncertainty in the track initiation process is rarely considered in the traditional track initiation methods.

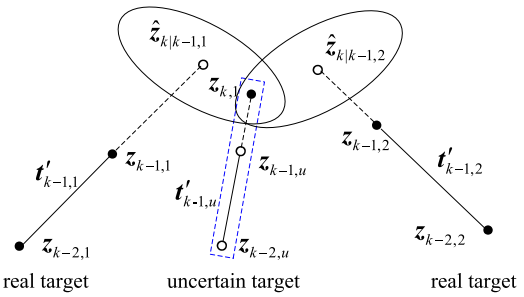

FIGURE 1. Crossing candidate temporary tracks.

C. ANALYZING THE ASSOCIATION UNCERTAINTY IN TRACK INITIATION

As discussed above, significant uncertainty exists in complex surveillance environments, such as the appearance of crossing targets and false targets. In addition, because of the limited performance of sensors, the uncertain motion patterns of a moving target, the uncertainty in the data processing of the tracking system and the dynamic interference from the surveillance environment, the measurements received by each sensor generally contain incomplete, uncertain and inconsistent information. These uncertain measurements also cause the uncertain association with different targets in the track initiation process.

To reduce the association uncertainty in the track initiation process, the neutrosophic set is introduced to describe the uncertain association in track initiation. Based on the neutrosophic set, the sources of measurements or clutters can be divided into three classes: real targets, uncertain targets and false targets. These targets can be further expressed by using the different sets as follows:

$$S = R \cup B \cup Z \tag{5}$$

where S denotes the set of the sources corresponding to all the targets in the surveillance field and R, B and Z denote the sets of real targets, uncertain targets and false targets, respectively. Hence, any a measurement may be associated with a real target, an uncertain target, or a false target.

Here, an example is presented to illustrate the uncertain association of a measurement with different targets as shown in Fig. 1. In Fig. 1, $\boldsymbol{t}'_{k-1,1}$ and $\boldsymbol{t}'_{k-1,2}$ are two candidate temporary tracks at $k-1$; $z_{k|k-1,1}$ and $z_{k|k-1,2}$ are their predicted positions, respectively; $z_{k-1,u}$ is the midpoint between $z_{k-1,1}$ and $z_{k-1,2}$; $z_{k-2,u}$ is the midpoint between $z_{k-2,1}$ and $z_{k-2,2}$. Measurement $z_{k,1}$, which is received by a sensor at k drops in the association gates of $\boldsymbol{t}'_{k-1,1}$ and $\boldsymbol{t}'_{k-1,2}$. For this uncertain association, one must consider not only the corresponding association degrees of $z_{k,1}$ belonging to $\boldsymbol{t}'_{k-1,1}$ and $\boldsymbol{t}'_{k-1,2}$ but also its association degree with regards to the uncertain candidate temporary track $\boldsymbol{t}'_{k-1,u}$. Here, $\boldsymbol{t}'_{k-1,u}$ is similarly defined as the set of $z_{k-1,u}$ and $z_{k-2,u}$ according to Eq. (4). In addition, $z_{k,1}$ is also possible from a false target.

This analysis of the uncertain association in the track initiation process shows that employing the neutrosophic set to describe the uncertain association is reasonable and feasible in the complex situation.

III. NEUTROSOPHIC HOUGH TRANSFORM

To avoid large traversal operations and reduce the association uncertainty between measurements and targets, the NHT method is developed based on the standard HT method.

A. STANDARD HOUGH TRANSFORM METHOD USING CANDIDATE TEMPORARY TRACKS

The basic concept of the HT is to transform a measurement (x_k, y_k) from the observation space (Cartesian space) to the parameter space (ρ, θ) by

$$\rho(\theta) = x_k \cos\theta + y_k \sin\theta \tag{6}$$

where x_k and y_k are the positions of a target in the x-axis and y-axis, respectively; ρ is the perpendicular distance between the point of the intersection of the line perpendicular to the line and the origin; and θ ($\theta \in [0, \pi]$) is the angle between this perpendicular line and the x-axis. Based on Eq. (6), each measurement (x_k, y_k) corresponds to a sine curve in the parameter space. Thus, by voting on the corresponding vote cells in the accumulation matrix, one can detect the peaks of the accumulation matrix and then determine the corresponding straight-line tracks. Fig. 2 shows the mapping relationship between the measurements and sine curves. If three measurements are located on a straight line, then their corresponding sine curves should intersect at a common parameter point. Hence, the HT can be employed for the track initiation of straight-line tracks in the MTT.

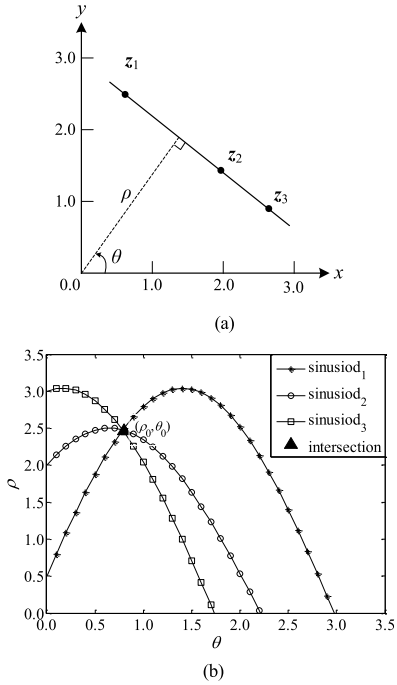

FIGURE 2. Relationship between the measurements and the sine curves. (a) Three measurements on a common line. (b) Three corresponding sine curves.

According to Eq. (6), two measurements can determine a parameter point in the parameter space, which is the intersection point of their corresponding sine curves in the valid interval of θ. Therefore, each candidate temporary track $\boldsymbol{t}'_{k,1} = \{z_{k-1,1}, z_{k,1}\}$ can be employed to directly calculate the corresponding parameter point (ρ, θ). Concretely can first determine the corresponding curves in the parameter space by Eq. (6) as follows

$$\rho(\theta) = x_{k-1}\cos\theta + y_{k-1}\sin\theta \tag{7}$$

$$\rho(\theta) = x_{k,1}\cos\theta + y_{k,1}\sin\theta \tag{8}$$

By solving Eqs. (7) and (8), the parameter point (ρ, θ) in the parameter space corresponding to the temporary candidate track consisting of two measurements $z_{k-1,1}$ and $z_{k,1}$ in the parameter space can be obtained

$$\theta = \begin{cases} -\arctan(\alpha_k) & \alpha_k > 0 \\ -\arctan(\alpha_k) + \pi & \alpha_k \leq 0 \end{cases} \tag{9}$$

$$\rho = \frac{\left| x_{k,1} y_{k-1,1} - x_{k-1,1} y_{k,1} \right|}{d(z_{k-1,1}, z_{k,1})} \tag{10}$$

Here, $d(z_{k-1,1}, z_{k,1})$ is the distance between measurements $z_{k-1,1}$ and $z_{k,1}$, α_k and $d(z_{k,1}, z_{k-1,1})$ can be calculated by

$$\alpha_k = \frac{x_{k,1} - x_{k-1,1}}{y_{k,1} - y_{k-1,1}} \tag{11}$$

$$d(z_{k-1,1}, z_{k,1}) = \sqrt{(x_{k,1}-x_{k-1,1})^2 + (y_{k,1}-y_{k-1,1})^2} \quad (12)$$

where $x_{k-1,1}$ and $y_{k-1,1}$ is the corresponding positions of measurement $z_{k-1,1}$ in the x-axis and y-axis, $x_{k,1}$ and $y_{k,1}$ is the corresponding positions of measurement $z_{k,1}$ in the x-axis and y-axis.

The parameter points calculated by Eqs. (9) and (10) can be utilized as the vote cells in the global accumulation matrix. Hence, using a candidate temporary track can avoid large traversal operations and then significantly reduce the vote times.

B. NEUTROSOPHIC HOUGH TRANSFORM METHOD USING CANDIDATE TEMPORARY TRACKS

Generally, the track of a moving target in the track initiation phase is assumed to be a straight line. Thus, the measurements from this target are theoretically located on a straight line. Due to the effects of noises and clutters in a complex tracking situation, these measurements are actually located around the straight line in the observation space, and their sine curves do not intersect at a common point in the parameter space. This effect can easily cause the peaks of the accumulation matrix to diverge and decline. Although the FHT can overcome the uncertainty problem somewhat [19], it is difficult to utilize the fuzzy set to describe the uncertain association of a measurement with different targets in a complex environment, such as the appearances of crossing targets and close targets.

To solve this problem, the NHT method is developed in the framework of the HT method. The main procedures of the NHT method are given as follows: i) first, a neutrosophic set is utilized to describe the uncertain association of a measurement with different targets including real targets, uncertain targets and false targets; ii) then, candidate temporary tracks are defined to calculate the parameter points in the accumulation matrix; iii) moreover, the weights of these parameter points are calculated by a Gaussian membership function based on the Euclidean distance of the parameter points to the straight lines (corresponding to the candidate temporary tracks); iv) these weights are further used for the counts of the corresponding vote cells in the accumulation matrix; v) finally, the peaks of the accumulation matrix are used to determine the real tracks.

As discussed above, the uncertain association in track initiation can be divided into three classes according to Eq. (6). Namely, a measurement may belong to a real target, an uncertain target or a false target. Using the neutrosophic set, their corresponding association degrees can be expressed as follows:

$$z_l \xrightarrow{NHT} \tilde{A}(\rho_i, \theta_i) \quad (13)$$

$$\tilde{A}(\rho_i, \theta_i) = \{<(\rho_i, \theta_i), \mu_I(\rho_i, \theta_i), \mu_F(\rho_i, \theta_i)> | (\rho_i, \theta_i) \in U\} \quad (14)$$

where $\tilde{A}$ is a neutrosophic set defined in the parameter space U; $\mu_T(\rho_i, \theta_i)$, $\mu_I(\rho_i, \theta_i)$ and $\mu_F(\rho_i, \theta_i)$ denote the membership functions to calculate the associate degree of a measurement with a real target, an uncertain target and a false target respectively, which can be defined by the Gaussian membership function as the following form:

$$\mu(\rho_i, \theta_i) = \exp\left[-\frac{(\rho_i-\rho_o)^2}{2\varepsilon_\rho^2}\right] \exp\left[-\frac{(\theta_i-\theta_o)^2}{2\varepsilon_\theta^2}\right] \quad (15)$$

where (ρ_i, θ_i) and(ρ_o, θ_o) are two parameter points in the parameter space, (ρ_i, θ_i) lies in the neighborhood $\sigma(\rho_i, \theta_i)$ of (ρ_o, θ_o), and ε_ρ and ε_θ are the given ρ-axis and θ-axis tolerance errors, respectively. These parameters are further illustrated in Subsection B of Section IV.

Based on Eq. (15), three local accumulation matrixes for the three classes of targets can be expressed by

$$C_T(\rho, \theta) = \sum\nolimits_U < \mu_T(\rho_i, \theta_i) > /(\rho_i, \theta_i) \quad (16)$$

$$C_I(\rho, \theta) = \sum\nolimits_U < \mu_I(\rho_i, \theta_i) > /(\rho_i, \theta_i) \quad (17)$$

$$C_F(\rho, \theta) = \sum\nolimits_U < \mu_F(\rho_i, \theta_i) > /(\rho_i, \theta_i) \quad (18)$$

Here, $\mu_T(\rho_i, \theta_i)$, $\mu_I(\rho_i, \theta_i)$ and $\mu_F(\rho_i, \theta_i)$ denote the existing probabilities of point (ρ_i, θ_i) in the corresponding local parameter space, and Σ denotes the list of all the parameter points.

To describe the existence probability of each parameter point in the global parameter space, one must design a logic rule for the inverse transform of the peaks of the accumulation matrix from the global parameter space to the observation space and the detection of straight-line tracks.

Logic rule: if measurement z_k is located on a straight-line track (ρ_i, θ_i) in the observation space, and (ρ_i, θ_i) exists in the local parameter space, **then** measurement z_k must belong to this straight-line track (ρ_i, θ_i) in the observation space, and (ρ_i, θ_i) must exist in the global parameter space, $i = 1, 2, \cdots, |C|$, where $|C|$ is the number of straight-line tracks in the global parameter space, and C is the global accumulation matrix.

Based on this reasoning rule, the global accumulation matrix can be defined as follows.

$$C(\rho, \theta) = \max\{C_T(\rho, \theta), C_I(\rho, \theta), C_F(\rho, \theta)\} \quad (19)$$

Thus, the value of each parameter point (ρ_i, θ_i) in the global parameter space that is greater than the given threshold, denotes the parameters of a straight-line track, $i = 1, 2, \cdots, |C|$.

IV. NEUTROSOPHIC HOUGH TRANSFORM-BASED TRACK INITIATION

Based on the analysis presented in Sections II and III, the NHT-TI method is developed as follows.

A. APPLYING CONSTRAINT CONDITIONS FOR CANDIDATE TEMPORARY TRACKS

To suppress false tracks and reduce vote times, two constraint conditions related to the velocity information of moving targets and the time information of measurement sequences are introduced in the NHT-TI.

Condition 1 (Velocity Constraint): Considering the velocity constraint of moving targets, the distance $d(\boldsymbol{z}_{k-1,i}, \boldsymbol{z}_{k,j})$ between any two measurements $\boldsymbol{z}_{k-1,i}$ and $\boldsymbol{z}_{k,j}$ in a candidate temporary track $\boldsymbol{t}'_{k,l}$ should satisfy the following inequation:

$$v_{\min} t_d \leq d(\boldsymbol{z}_{k-1,i}, \boldsymbol{z}_{k,j}) \leq v_{\max} t_d \tag{20}$$

where $v_{\min}$ and $v_{\max}$ denote the minimum and the maximum admissible velocities for a moving target, respectively, and t_d is the time interval between two observations.

Condition 2 (Time Constraint): According to the time information of measurement sequences, there is a constraint for the candidate temporary track $\boldsymbol{t}'_{k,l}$ that needs to be transformed by the NHT:

$$\{\boldsymbol{t}_{k,i}\}_{i=1}^{M_k} \subseteq \{\boldsymbol{t}'_{k,l}\}_{l=1}^{M'_k} \subseteq \{\boldsymbol{t}'_{k,j}\}_{j=1}^{M''_k} \tag{21}$$

$$M_k \leq M'_k \leq M''_k \tag{22}$$

Here, $\boldsymbol{t}_{k,i}$ and $\boldsymbol{t}'_{k,j}$ denote a temporary track and a candidate temporary track, respectively, at time k; M_k, M'_k and M''_k denote the corresponding numbers of $\boldsymbol{t}_{k,i}, \boldsymbol{t}'_{k,l}$ and $\boldsymbol{t}'_{k,j}$, respectively; $M''_k = \mathrm{C}^1_{n_{k-1}} \mathrm{C}^1_{n_k}$; and n_{k-1} and n_k are the numbers of measurements observed by the sensor at $k-1$ and k, respectively.

From Eq. (21), each temporary track of a real target should belong to the set of candidate temporary tracks. Hence, all the tracks of real targets can be determined by detecting the peaks of the global accumulation matrix.

B. CALCULATING THE GLOBAL ACCUMULATION MATRIX

Assuming that a sensor receives measurement $\boldsymbol{z}_{k,i}$ at $k (k \geq 2)$, one can obtain all the candidate temporary tracks based on the combinations of $\boldsymbol{z}_{k,i}$ with each measurement at $k-1$, and then the global accumulation matrix C_k can be calculated based on Eqs. (10)-(13):

$$C_k(\rho_{k,i}, \theta_{k,i}) = \sum\nolimits_U \mu_C(\rho_{k,i}, \theta_{k,i}) / (\rho_{k,i}, \theta_{k,i}) \tag{23}$$

$$\mu_C\left(\rho_{k,i}, \theta_{k,i}\right) = \max\{\mu_T(\rho_{k,i}, \theta_{k,i}), \mu_I(\rho_{k,i}, \theta_{k,i}), \mu_F(\rho_{k,i}, \theta_{k,i})\} \tag{24}$$

where $i = 1, 2, \cdots, M'_k$, and M'_k is the number of parameter points corresponding to the candidate temporary tracks that satisfy the above constraint conditions described as above at k. In the detection process, the parameter space is divided into many discrete cells, and the center of each cell is calculated by the following equations:

$$\rho_{k,i} = \left(i - \frac{1}{2}\right) \Delta\rho, \quad i = 1, 2, \cdots, n_\rho \tag{25}$$

$$\theta_{k,i} = \left(i - \frac{1}{2}\right) \Delta\theta, \quad i = 1, 2, \cdots, n_\theta \tag{26}$$

where $\Delta\rho$ and $\Delta\theta$ are the corresponding sampling intervals in the ρ-axis and θ-axis, respectively. Additionally, $\Delta\rho = \rho_{\max}/n_\rho$, $\Delta\theta = \theta_{\max}/n_\theta$, and n_ρ and n_θ denote the sampling numbers.

In fact, the NHT does not directly distinguish whether a candidate temporary track is from a real target, or whether a parameter point in the parameter space corresponds to the real target. Thus, the peaks of the global accumulation matrix must be identified to determine the real tracks. Each parameter point $(\rho_{k-1,\mathrm{o}}, \theta_{k-1,\mathrm{o}})$ that was generated at the previous time is set to a kernel point (assuming that it corresponds to a real target), and each parameter point $(\rho_{k,i}, \theta_{k,i})$ generated at the current time is set to a non-kernel point, $\mathrm{o} = 1, 2, \cdots, N_k$, $i = 1, 2, \cdots, M'_k$. The existence probabilities of the kernel points are initialized as $1 - P_F$ and those of the non-kernel points are calculated by the Gaussian membership function based on Eq. (15). Here, P_F is assumed to be the false alarm rate of the sensor. Based on this analysis, the membership function in Eq. (15) can be further modified as follows

$$\mu(\rho_{k,i}, \theta_{k,i}) = \exp\left[-\frac{(\rho_{k,i} - \rho_{k-1,\mathrm{o}})^2}{2\varepsilon_\rho^2}\right] \exp\left[-\frac{(\theta - \theta_{k-1,\mathrm{o}})^2}{2\varepsilon_\theta^2}\right] \tag{27}$$

where $(\rho_{k,i}, \theta_{k,i}) \in \sigma(\rho_{k-1,\mathrm{o}}, \theta_{k-1,\mathrm{o}})$, $\mathrm{o} = 1, 2, \cdots, M'_{k-1}$, $i = 1, 2, \cdots, M'_k$, $\sigma(\rho_{k,i}, \theta_{k,i})$ denotes the neighborhood of the kernel point $(\rho_{k,\mathrm{o}}, \theta_{k,\mathrm{o}})$ expressed by

$$\sigma\left(\rho_{k-1,\mathrm{o}}, \theta_{k-1,\mathrm{o}}\right) = \left[\rho_{k-1,\mathrm{o}} - 2\varepsilon_\rho\right] \times \left[\theta_{k-1,\mathrm{o}} - 2\varepsilon_\theta\right] \tag{28}$$

Consequently, by combining Eq. (27) with Eqs. (16), (17) and (18), one can obtain $C_T(\rho, \theta)$, $C_N(\rho, \theta)$ and $C_F(\rho, \theta)$, respectively.

Assuming that the false alarm rate P_F of a sensor is given as discussed above, each candidate temporary track $\boldsymbol{t}'_{k,i}$ is a possible false target generated by a clutter, and its corresponding membership degree is calculated by the following equation:

$$F_{k,i} = \lambda_k P_F^2 \tag{29}$$

where λ_k is an adjustment factor. In addition, because each measurement corresponds to at most a single target at most, its membership functions with a real target, an uncertain target and a false target must satisfy the following equation:

$$\mu_T(\rho_{k,i}, \theta_{k,i}) + \mu_N(\rho_{k,i}, \theta_{k,i}) + \mu_F(\rho_{k,i}, \theta_{k,i}) = 1 \tag{30}$$

In n successive observation times, all the measurements received by a sensor at each time can used to calculate the weight of the corresponding vote cell in the global accumulation matrix according to Eq. (24), and then the global accumulation matrix C corresponding to real targets can be further expressed by

$$C(\rho, \theta) = \sum\nolimits_{t=k-1}^{k-2+n} \sum\nolimits_i \mu_F(\rho, \theta) \delta(\rho - \rho_i) \delta(\theta - \theta_i) \tag{31}$$

where $\delta(\cdot)$ is the Dirac function. Hence, the probability $\tilde{C}(\rho, \theta)$ that the parameter point (ρ, θ) exists in the global space can be expressed by normalizing $C(\rho, \theta)$.

$$\tilde{C}_k(\rho, \theta) = C_k(\rho, \theta) / \max(C_k(\rho, \theta)) \tag{32}$$

Assuming the value of the affirming gate is set to $\boldsymbol{\tau}_{\tilde{C}}$, if $\tilde{C}_{\boldsymbol{k}}(\boldsymbol{\rho}, \boldsymbol{\theta}) \geq \boldsymbol{\tau}_{\tilde{C}}$, then the target corresponding to point $(\boldsymbol{\rho}, \boldsymbol{\theta})$ exists; when $\tilde{C}_{\boldsymbol{k}}(\boldsymbol{\rho}, \boldsymbol{\theta}) < \boldsymbol{\tau}_{\tilde{C}}$, the target does not exist. The main procedures of the NHT-TI method are given as shown in Fig. 3.

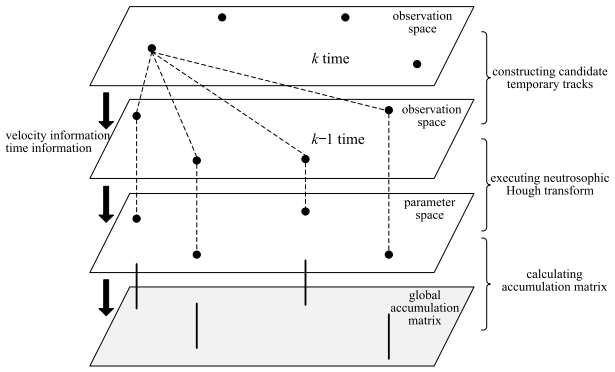

FIGURE 3. Main procedures of the NHT-TI method.

V. EXPERIMENTAL RESULTS AND ANALYSIS

Two experiments with simulated data and real data have been conducted to evaluate the performance of the proposed NHT-TI method in comparison with the standard HT-TI method, the modified HT-TI (MHT-TI) method and the improved HT-TI (IHT-TI) method mentioned in Section I in terms of the detection results and the average run time. The experiments are conducted by using a computer with a dual-core CPU of Core(TM) i5-6300 at 2.93 GHz with 8-GB of RAM. The programs of four track initiation methods are implemented by using MATLAB 2014b version software.

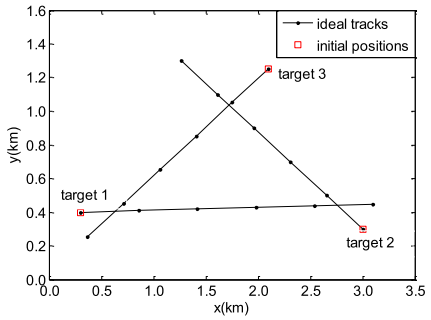

FIGURE 4. Ideal tracks.

TABLE 1. Initial states of three targets.

No.	Initial state of each target
Target 1	(300 m, 280.0 m/s, 400 m, 49.0 m/s)$^{\mathrm{T}}$
Target 2	(3000 m, -173.2 m/s,300 m, -100.0 m/s)$^{\mathrm{T}}$
Target 3	(2100 m, -173.2 m/s,1300 m, -100.0 m/s)$^{\mathrm{T}}$

A. SIMULATED DATA EXPERIMENT

In the simulation scenario, four initial situations were designed to evaluate the performance of the four track initiation methods described above. As shown in Fig. 4, three crossing targets are moving with constant velocities and maintaining their flight of duration for 12 s in the surveillance area. The sampling time of the sensor is 2 s. The initial states of the three targets are given in Table 1. In the simulation, the detection probability, the gate probability and the false alarm rate are set to $P_D = 0.99$, $P_G = 0.99$, and $P_F = 0.01$, respectively. The minimum and maximum velocities are set to $v_{\min} = 100$m/s and $v_{\max} = 400$m/s. The given ρ-axis and θ-axis tolerance errors are set to $\varepsilon_\rho = 20$ and $\varepsilon_\theta = 0.004$. The clutter model is assumed to follow a uniform distribution, and the number of clutters is assumed to follow a Poisson distribution with a known parameter $\lambda = 10$ (the number of clutters per unit of volume (km^2)). In addition, the sampling intervals on the ρ-axis and θ-axis are set to $\Delta\rho = 5$m and $\Delta\theta = 0.001$rad, respectively. The ideal tracks (without noises and clutters) and the noisy tracks (with noises and clutters) are as shown in Figs. 4 and 5, respectively. The initialized tracks obtained by the NHT-TI method are given in Fig. 6. These tracks have been further updated by the recursive least squares filter (RLSF) [28].

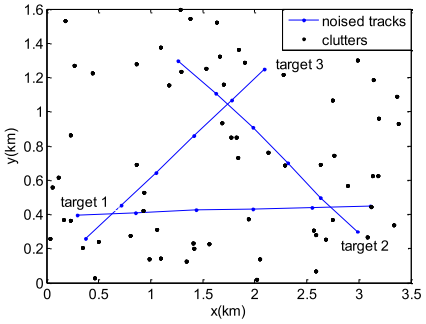

FIGURE 5. Noisy tracks in the cluttered situation.

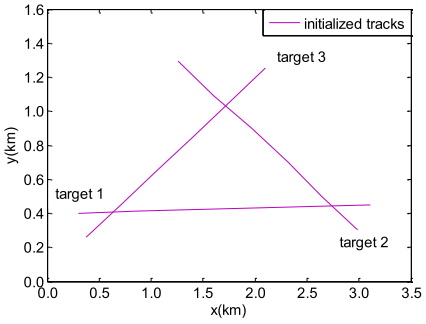

FIGURE 6. Initialized tracks.

The target state model and the measurement model are respectively expressed by

$$\boldsymbol{x}_k = \begin{bmatrix} 1 & T & 0 & 0 \\ 0 & 1 & 0 & 0 \\ 0 & 0 & 1 & T \\ 0 & 0 & 0 & 1 \end{bmatrix} \boldsymbol{x}_{k-1} + \begin{bmatrix} T/2 & 0 \\ 1 & 0 \\ 0 & T/2 \\ 0 & 1 \end{bmatrix} \boldsymbol{w}_k \quad (33)$$

$$\boldsymbol{z}_k = \begin{bmatrix} 1 & 0 & 0 & 0 \\ 0 & 0 & 1 & 0 \end{bmatrix} \boldsymbol{x}_k + \boldsymbol{v}_k \quad (34)$$

where T denotes the sampling interval, $\boldsymbol{x}_k = [x_k \dot{x}_k y_k \dot{y}_k]^{\mathrm{T}}$ is the state vector, x_k and y_k denote the positions of a target in the x-axis and y-axis, respectively, and $\dot{x}_k$ and $\dot{y}_k$ denote the corresponding velocities. The process noise $\boldsymbol{w}_k$ is assumed to be the zero-mean Gaussian white noise with

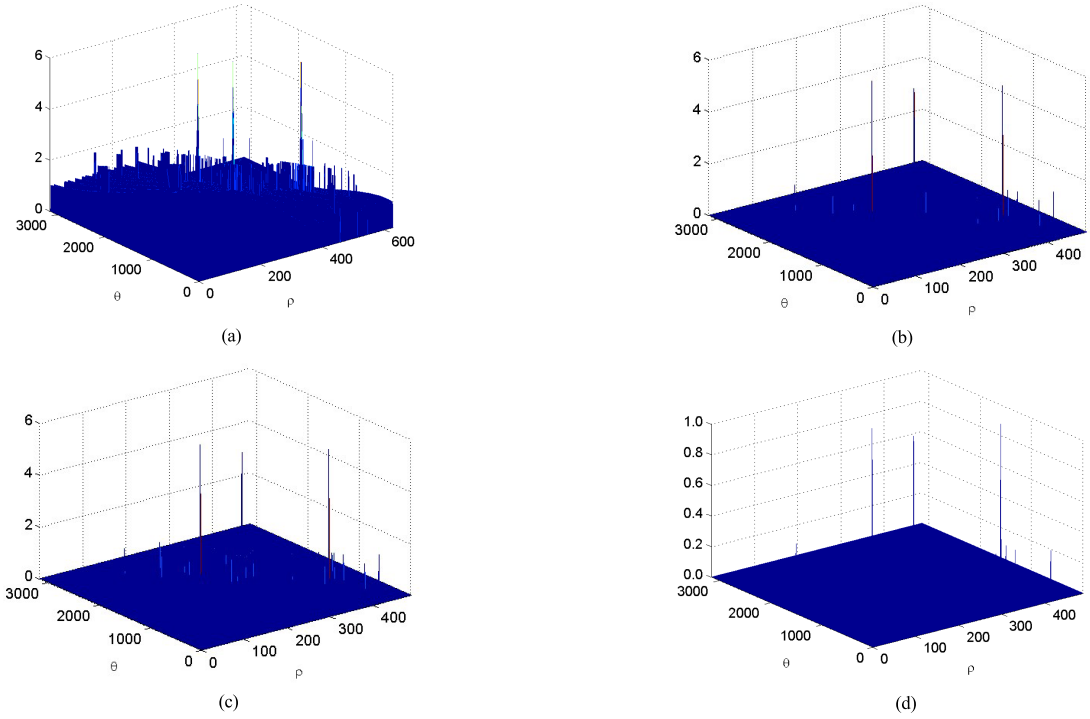

FIGURE 7. Detection results in the ideal situation without noises and clutters. (a) HT. (b) MHT. (c) IHT. (d) NHT.

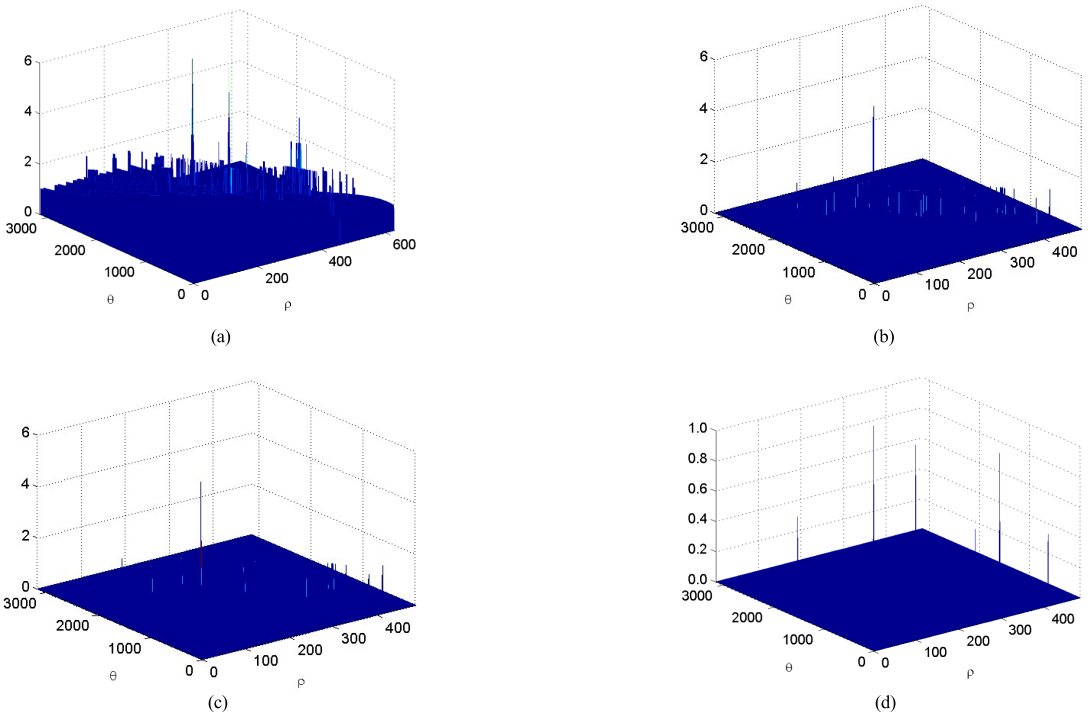

FIGURE 8. Detection results in the noisy situation without clutters. (a) HT. (b) MHT. (c) IHT. (d) NHT.

covariance $Q = \text{diag}\left(\left[0.01^2\text{km}^2\text{s}^4, 0.01^2\text{km}^2\text{s}^4\right]\right)$; that is $\boldsymbol{w}_k \sim N(0, Q)$. The measurement noise $\boldsymbol{v}_k$ is also assumed to be the zero-mean Gaussian white noise with covariance $R = \text{diag}([0.01^2\text{km}^2, 0.01^2\text{km}^2])$; namely, $\boldsymbol{v}_k \sim N(0, R)$.

Figs. 7-10 show the 3D histograms detected by using the four methods in the four situations, concretely including the ideal situation without noises and clutters (Situation I), the noisy situation without clutters (Situation II), the

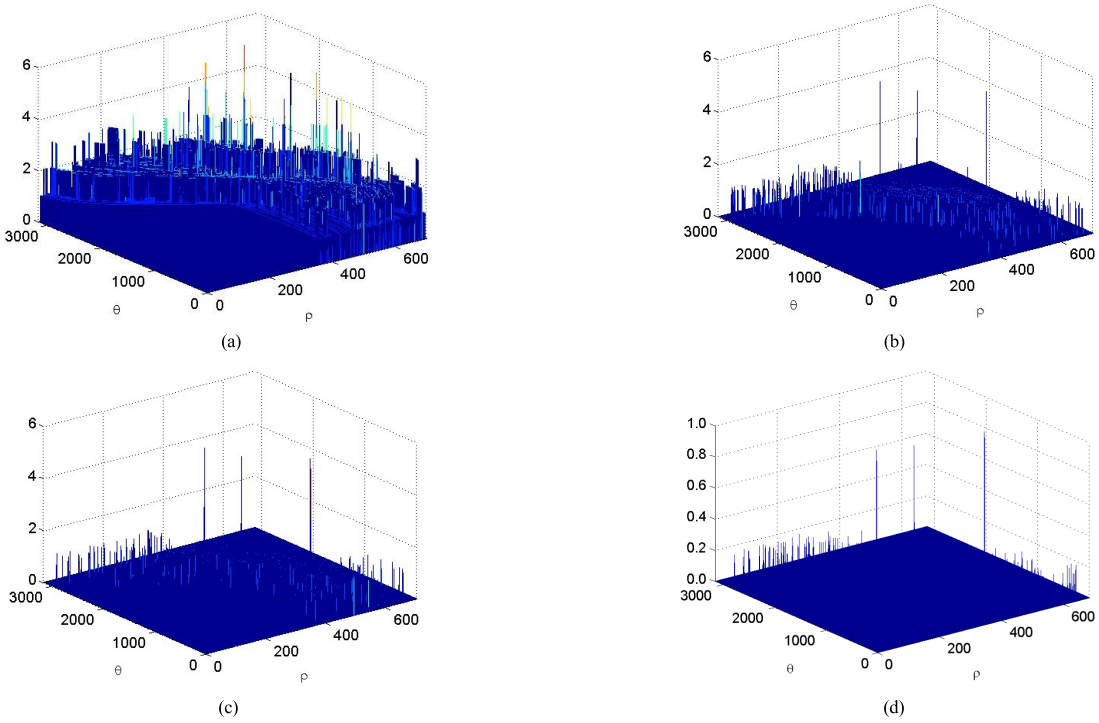

FIGURE 9. Detection results in the cluttered situation without noises. (a) HT. (b) MHT. (c) IHT. (d) NHT.

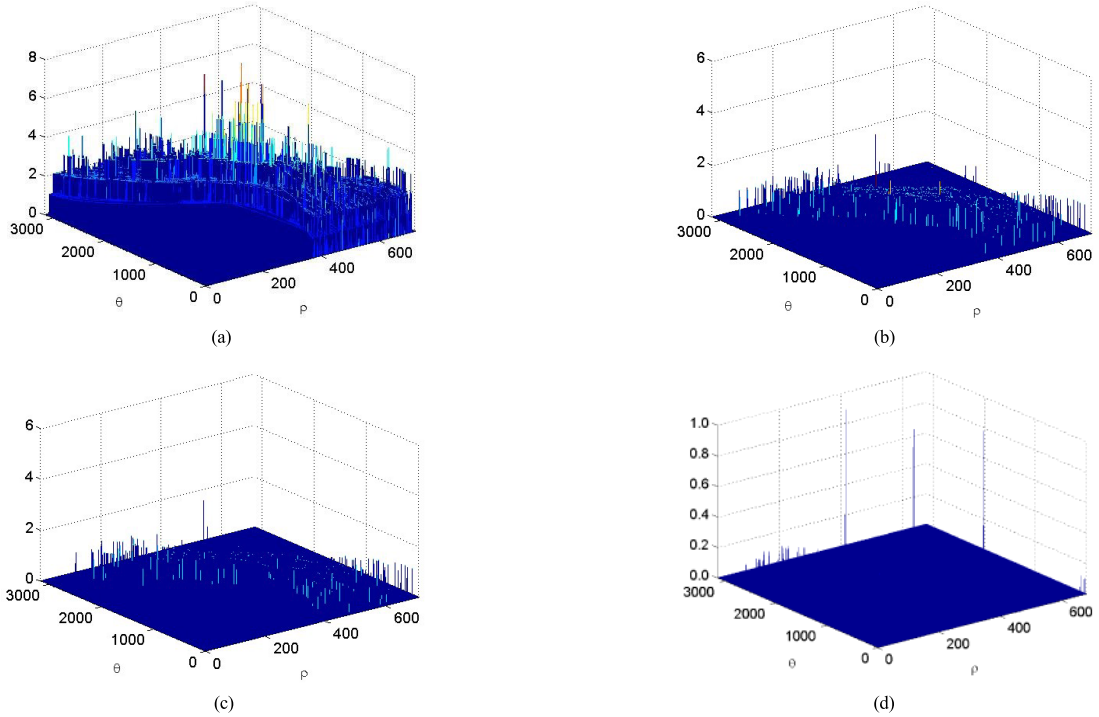

FIGURE 10. Detection results in the noisy and cluttered situation. (a) HT. (b) MHT. (c) IHT. (d) NHT.

cluttered situation without noises (Situation III), and the noisy and cluttered situation (Situation IV). The four methods are further compared in Table 2. The results show that the HT method performs well in the noisy situations but poorly in the cluttered situations, whereas the MHT method performs well in the cluttered situations but poorly in the noisy situations.

TABLE 2. Comparison of the performances of the four track initiation methods.

No.	Performance	HT	MHT	IHT	NHT
Situation I	discrimination	high	high	high	high
	divergence	slight	none	none	slight
	decline	none	slight	slight	slight
Situation II	discrimination	high	low	low	high
	divergence	slight	medium	medium	slight
	decline	slight	serious	serious	slight
Situation III	discrimination	low	high	high	high
	divergence	slight	slight	slight	slight
	decline	slight	slight	slight	slight
Situation IV	discrimination	low	low	low	high
	divergence	medium	serous	serous	slight
	decline	medium	serious	serious	slight

The IHT method acquire the approximative results in four situations, like the MHT method. The NHT method performs relatively well in both two classes of situations.

The performance of the four methods is further analyzed as follows. The HT method yields the good results in Situations I and II, as shown in Figs. 7(a) and 8(a), but its performance significantly decreases in Situations III and IV, as shown in Figs. 9(a) and 10(a). Specifically, the HT method performs well in the noisy situations but poorly in the cluttered situations. In the cluttered situations, the clutters can cause many false temporary tracks, these false temporary tracks further generate many parameter points in the parameter space. Because the HT method must execute the traversal operation for all the parameter points of each sampling $\Delta\theta$, large false peaks are introduced into the global accumulation matrix. Hence, the HT method consumes additional computational resources due to the clutters, and it is difficult to identify the peaks that correspond to the real targets in the cluttered situation. In addition, the peaks diverge to various extents because of the existence of measurement noises.

The MHT method obtains the satisfactory results in Situations I and III, as shown in Figs. 7(b) and 9(b), but its performance degrades seriously in Situations II and IV, as seen in Figs. 8(b) and 10(b). The MHT method performs well in the cluttered situations but poorly in noisy situations. Because the MHT method utilizes the candidate temporary tracks to directly calculate the weights for voting the parameter points, it can avoid large traversal operations, unlike the HT method, and reduce the computational burden and false peaks generated in the global accumulation matrix. Additionally, because the effect of measurement noises on the candidate temporary tracks used in the MHT method is greater than those of the single measurement used in the HT method, the performance of the MHT method is worse than that of the HT method in noisy situations. In addition, because the binary accumulation function employed by the MHT method cannot overcome the effect of measurement noises on the accumulation of the parameter points, it also causes the divergence and decline of the peaks corresponding to real targets. The IHT method can achieve the approximative results, like the MHT method, as shown in Figs. 7(c), 8(c), 9(c) and 10(c). Because the IHT method introduces the motion information to suppress the false candidate temporary tracks, it can reduce the times of HT. Therefore, it consumes less computational complexity than the MHT, as shown in Fig. 11.

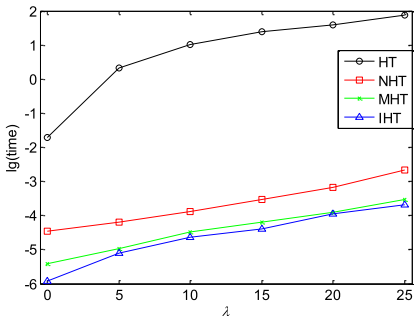

FIGURE 11. Average run times of the four methods.

The NHT method obtains good results in both the noisy situations and the cluttered situations, as shown in Figs. 7(d), 8(d), 9(d) and 10(d). Notably, the NHT method not only uses the candidate temporary tracks to modify the accumulation rule of the HT method but also employs the neutrosophic set to calculate the global accumulation matrix. Hence, the NHT method reduces the computational burden and suppresses the effect of measurement noises. Although a slight divergence and slight decline in the peaks of the global accumulation matrix occur in the noisy and cluttered situation, as shown in Fig. 7(d), the detected results are still adequate for identifying the parameter points corresponding to real targets from the noisy measurements and clutters. As a result, the performance of the NHT method is better those of the HT method and the MHT method, and it is more robust in complex environments for targets that are close and have crossing trajectories.

The average run times of the four methods are further utilized to illustrate their computational complexities (Fig. 11).

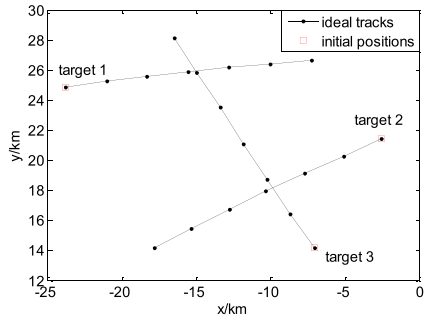

FIGURE 12. Ideal tracks.

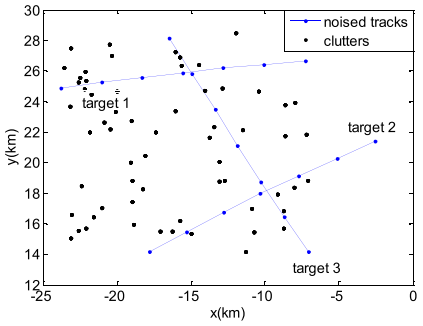

FIGURE 13. Noisy tracks in cluttered situation.

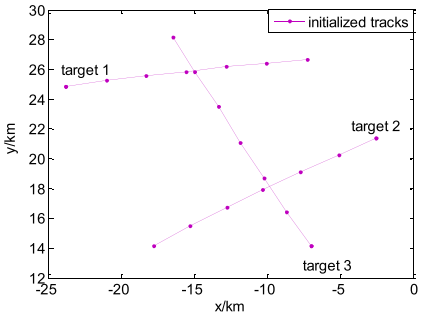

FIGURE 14. Initialized tracks.

For simplicity of comparison, we take the log of the average run times obtained by 50 Monte Carlo simulation runs in the situations with different clutter densities λ. The results show that the average run times of all the four methods increase with λ. The order of the four track initiation methods lists as the HT method, the NHT method, the MHT method and the IHT method according to the average run times from the most to the least. The average run time of the HT method is greater than those of the MHT method, the IHT method and the NHT method because the HT method must execute the large traversal operations for all the parameter points of each sampling $\Delta\theta$. In addition, compared with the MHT method and the IHT method, the NHT method requires additional time to execute the neutrosophic accumulation; as a result, its average run time is slightly greater than those of the MHT method and the IHT method. Because the IHT method introduce the motion information to suppress the false candidate temporary tracks, the average run time of the IHT method is less than that of the MHT method.

In summary, the proposed NHT method can effectively reduce the association uncertainty between measurements and different targets in the track initiation procedure of MTT and accurately detect the peaks corresponding to real targets in complex environments where the targets are close and crossing. Hence, the NHT method is more robust for track initiation than the HT method, the MHT method and the IHT method in complex environments. In addition, the NHT method can avoid large traversal operations, thereby reducing the computational complexity.

B. REAL DATA EXPERIMENT

To illustrate the feasibility of the proposed NHT-TI method, an experiment with real data is employed to evaluate its performance by using the real tracking data generated from a type of single radar. The real data set consists of three crossing tracks. Each track consists of seven periodic track dots, and the flying times of duration for 70 s are maintained in the surveillance area as shown in Fig. 12. The sampling interval T of the radar is 10 s. The sampling intervals on the ρ-axis and θ-axis are set to $\Delta\rho = 5$ m and $\Delta\theta = 0.001$rad, respectively. The radar measurements of the three targets at each sampling time are given in Table 3. In the real data experiment, the detection probability, the gate probability and the false alarm rate are set to $P_D = 0.99$, $P_G = 0.99$, and $P_F = 0.01$, respectively. The minimum and maximum velocities are set to $v_{\min} = 100$m/s and $v_{\max} = 400$m/s. The given ρ-axis and θ-axis tolerance errors are set to $\varepsilon_\rho = 20$ and $\varepsilon_\theta = 0.004$. The clutter model is assumed to follow a uniform distribution, and the number of clutters is assumed to follow a Poisson distribution with a known parameter $\lambda = 10$ (the number of clutters per unit of volume (km^2)). Based on the analysis results for different situations in the simulated data experiment described above, only the noisy and cluttered situation is considered here. Fig. 13 shows the noisy tracks in the cluttered situation, and Fig. 14 shows the initialized tracks generated by the proposed NHT-TI method that have been filtered by the RLSF method. Figure 15 shows the detection results of the four track initiation methods in the noisy and cluttered situation.

TABLE 3. Radar measurements of three targets.

No.	Target 1(m)	Target 2 (m)	Target 3 (m)
Time 1	(-23793, 24841)	(-2548,21411)	(-7021,14156)
Time 2	(-21011,25246)	(-5080,20251)	(-8675,16448)
Time 3	(-18300,25575)	(-7720,19125)	(-10248,18720)
Time 4	(-15547,25858)	(-10322,17938)	(-11849,21086)
Time 5	(-12823,26185)	(-12766,16739	(-13363,23508)
Time 6	(-10050,26402)	(-15310,15467)	(-14961,25823)
Time 7	(-7248,26643)	(-17794,14169)	(-16459,28155)

The performances of the four track initiation methods are further analyzed as follows. Fig. 15 shows that the HT method, the MHT method and the IHT method are unable to identify the peaks corresponding to real targets, and their detected results significantly diverge and decline in accuracy. Although the peaks detected by the NHT method also diverge

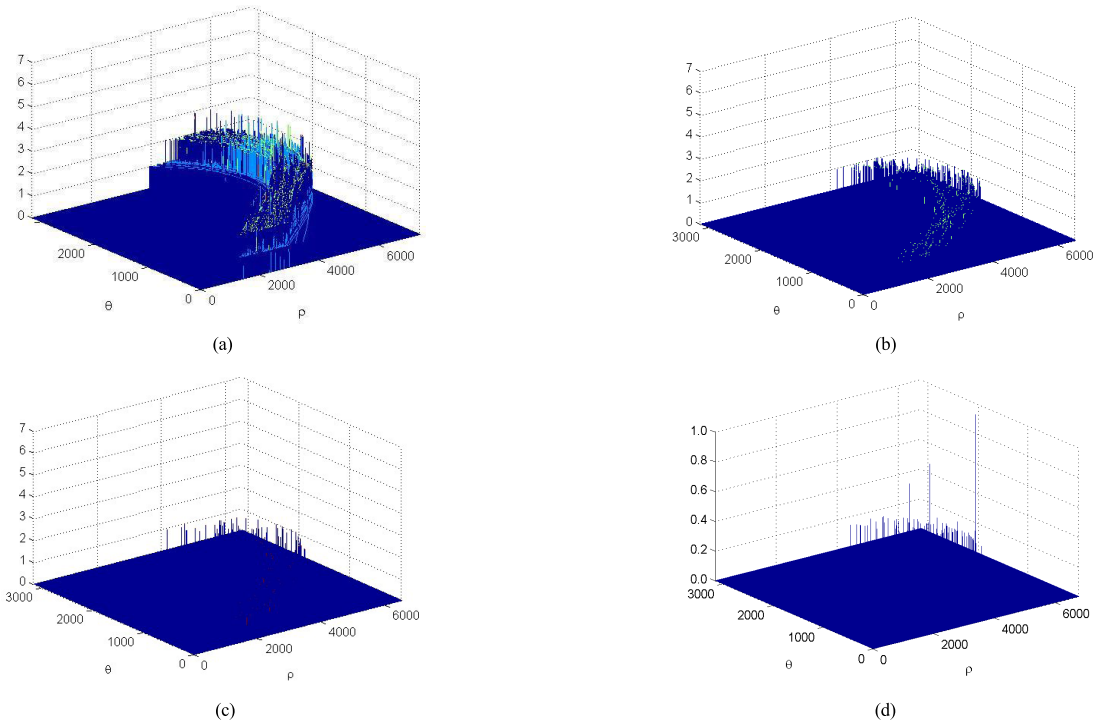

FIGURE 15. Detection results in the noisy and cluttered situation. (a) HT. (b) MHT. (c) IHT. (d) NHT.

and decline to an extent, the approach can still identify the peaks corresponding to the three real targets and obtain their initialized tracks (Fig. 14). Furthermore, the average run times of the HT method, the NHT method, the MHT method and the IHT method for 50 Monte Carlo runs are 4.0209 s, 0.1330 s, 0.0637 s and 0.0518 s, respectively. The average run time of the HT is more than those of the NHT method, the MHT method and the IHT method, and the average run time of the latter two are approximatively equal. These results are consistent with the discussed results for the computational complexity of the four methods in the simulated data experiment discussed above.

The experiment with real data verified that the proposed NHT-TI method is feasible in a real complex environment, and its performance is better than those of the HT method, the MHT method and the IHT method.

VI. CONCLUSION

In this paper, the characteristics of the traditional HT-TI methods were analyzed in different tracking situations, and then the NHT-TI method was proposed to solve the uncertain track initiation problem in complex surveillance environments. In the proposed NHT-TI method, the uncertain association of a measurement with different targets is classified as the association with real targets, uncertain targets and false targets. Due to the advantage of the neutrosophic set theory in describing and processing uncertain information, the neutrosophic set is employed to describe the uncertain association of a measurement with the three different targets described above. Moreover, the NHT method was developed in the framework of the standard HT method. Based on the sequential processing mode of the sensors, candidate temporary tracks were defined to calculate the parameter points in the parameter space, and then these parameter points were utilized to vote for the global accumulation matrix based on the Gaussian membership function. Hence, the proposed NHT-TI method can avoid large traversal operations and significantly reduce computational complexity. Finally, the real targets were identified by detecting the peaks of the global accumulation matrix through an inverse transform.

In addition, two constraint conditions related to the motion information of moving targets and the time information of measurement sequences were introduced in the definition of candidate temporary tracks to suppress false tracks and reduce the vote times. Based on the facts described above, the effects of noises and clutters were also considered and analyzed in the NHT method. The results of experiments with simulated data and real data illustrated the effectiveness and feasibility of the proposed NHT-TI method, which exhibited better performance in terms of the correct detection rate and computational complexity for straight-line tracks than the standard HT-TI method, the MHT-TI method and the IHT-TI method. In future work, we will further study the effects of measurement noise and parameter space partitioning on the detection results of the proposed NHT-TI method.

REFERENCES

[1] H. Benoudnine *et al.*, "Real time Hough transform based track initiators in clutter," *Inf. Sci.*, vols. 337–338, pp. 82–92, Apr. 2016.

[2] B. Khaleghi, A. Khamis, F. O. Karray, and S. N. Razavi, "Multisensor data fusion: A review of the state-of-the-art," *Inf. Fusion*, vol. 14, no. 1, pp. 28–44, 2013.
[3] G. Sahin and M. Demirekler, "A multi-dimensional Hough transform algorithm based on unscented transform as a track-before-detect method," in *Proc. 17th Int. Conf. Inf. Fusion*, Salamanca, Spain, Jul. 2014, pp. 1–8.
[4] X. Bi, J. Du, Q. Zhang, and W. Wang, "Improved multi-target radar TBD algorithm," *J. Syst. Eng. Electron.*, vol. 26, no. 6, pp. 1229–1235, Dec. 2015.
[5] C. Qiu, Z. Zhang, H. Lu, and H. Luo, "A survey of motion-based multi-target tracking methods," *Prog. Electromagn. Res.*, vol. 62, pp. 195–223, Mar. 2015.
[6] Y. Bar-Shalom and X. R. Li, "Effectiveness of the likelihood function in logic-based track formation," *IEEE Trans. Aerosp. Electron. Syst.*, vol. 27, no. 1, pp. 184–187, Jan. 1991.
[7] T. Furukawa, F. Muraoka, and Y. Kosuge, "Multi-target and multi-sensor data fusion by rule-based tracking methodology," in *Proc. 37th SICE Annu. Conf.*, Chiba, Japan, Jul. 1998, pp. 1005–1012.
[8] H. Leung, Z. Hu, and M. Blanchette, "Evaluation of multiple target track initiation techniques in real radar tracking environments," *IEE Proc.-Radar, Sonar Navigat.*, vol. 143, no. 4, pp. 246–254, Aug. 1996.
[9] Z. Wu, J. Zhang, L. Zhang, and C. Tian, "A novel Hough track initialization algorithm for multi-sensor environment," *Sensor Lett.*, vol. 11, no. 4, pp. 686–691, Apr. 2013.
[10] L. R. Moyer, J. Spak, and P. Lamanna, "A multi-dimensional Hough transform-based track-before-detect technique for detecting weak targets in strong clutter backgrounds," *IEEE Trans. Aerosp. Electron. Syst.*, vol. 47, no. 4, pp. 3062–3068, Oct. 2011.
[11] C. G. Hempel, "Sequential track initialization with page's test," *IEEE Trans. Aerosp. Electron. Syst.*, vol. 46, no. 1, pp. 414–424, Jan. 2010.
[12] P. V. C. Hough, "Method and means for recognizing complex patterns," U.S. Patent 3 069 654, Mar. 25, 1960.
[13] M. Smith, "Feature space transform for multitarget detection," in *Proc. 19th IEEE Conf. Decision Control Including Symp. Adapt. Process.*, Albuquerque, NM, USA, Dec. 1980, pp. 835–836.
[14] M. Godec, P. M. Roth, and H. Bischof, "Hough-based tracking of non-rigid objects," *Comput. Vis. Image Understand.*, vol. 117, no. 10, pp. 1245–1256, Oct. 2013.
[15] J. Climent and R. A. Hexsel, "Particle filtering in the Hough space for instrument tracking," *Comput. Biol. Med.*, vol. 42, no. 5, pp. 614–623, May 2012.
[16] O. Khayat, M. Ghergherehchi, H. Afarideh, S. A. Durrani, A. A. Pouyan, and Y. S. Kim, "ATMS software: Fuzzy Hough transform in a hybrid algorithm for counting the overlapped etched tracks and orientation recognition," *Radiat. Meas.*, vol. 50, pp. 249–252, Mar. 2013.
[17] J. H. Han, L. T. Kóczy, and T. Poston, "Fuzzy Hough transform," *Pattern Recognit. Lett.*, vol. 15, pp. 649–658, Jul. 1994.
[18] N. Suetake, E. Uchino, and K. Hirata, "Generalized fuzzy Hough transform for detecting arbitrary shapes in a vague and noisy image," *Soft Comput.*, vol. 10, no. 12, pp. 1161–1168, Oct. 2006.
[19] O. Strauss, "Use the fuzzy Hough transform towards reduction of the precision/uncertainty duality," *Pattern Recognit.*, vol. 32, no. 11, pp. 1911–1922, Dec. 1999.
[20] F. Smarandache, *A Unifying Field in Logics. Neutrosophy: Neutrosophic Probability, Set and Logic*. Rehoboth, DE, USA: American Research Press, 1999.
[21] Y. Guo and A. Sengur, "NCM: Neutrosophic *c*-means clustering algorithm," *Pattern Recognit.*, vol. 48, no. 8, pp. 2710–2724, Aug. 2015.
[22] J. Ye, "A multicriteria decision-making method using aggregation operators for simplified neutrosophic sets," *J. Intell. Fuzzy Syst.*, vol. 26, no. 5, pp. 2459–2466, Sep. 2014.
[23] M. Zhang, L. Zhang, and H. D. Cheng, "A neutrosophic approach to image segmentation based on watershed method," *Signal Process.*, vol. 90, no. 5, pp. 1510–1517, May 2010.
[24] K. L. Hu, J. Ye, E. Fan, L. J. Huang, and J. T. Pi, "A novel object tracking algorithm by fusing color and depth information based on single valued neutrosophic cross-entropy," *J. Intell. Fuzzy Syst.*, vol. 32, no. 3, pp. 1775–1786, Feb. 2017.
[25] J. Ye, "Single-valued neutrosophic similarity measures based on cotangent function and their application in the fault diagnosis of steam turbine," *Soft Comput.*, vol. 21, no. 3, pp. 817–825, Feb. 2017.
[26] M. Arora and R. Biswas, "Deployment of neutrosophic technology to retrieve answer for queries posed in natural language," in *Proc. 3rd IEEE Int. Conf. Comput. Sci. Inf. Technol. (ICCSIT)*, Chengdu, China, Jul. 2010, pp. 435–439.
[27] J. Liu, Y. Liu, and W. Xiong, "A novel track initiation method based on prior motion information and Hough transform," in *Proc. Int. Conf. Intell. Inf. Process.*, Melbourne, VIC, Australia, Nov. 2016, pp. 72–77.
[28] E. Fan, W.-X. Xie, and Z.-X. Liu, "Maneuvering target tracking using fuzzy logic-based recursive least squares filter," *EURASIP J. Adv. Signal Process.*, vol. 2014, p. 53, Dec. 2014.

EN FAN received the B.S. degree in electronic information science and technology from Hubei Engineering University in 2002, the M.S. degree in signal and information processing from Nanchang Hangkong University in 2006, and the Ph.D. degree in signal and information processing from Xidian University in 2015. He is currently a Post-Doctoral Researcher with Shenzhen University and a Lecturer with Shaoxing University. His current research interests include multiple target tracking and data fusion.

WEIXIN XIE received the B.S. degree from Xidian University, Xi'an. He was a Faculty Member with Xidian University in 1965. From 1981 to 1983, he was a Visiting Scholar with the University of Pennsylvania, USA, where he was a Visiting Professor in 1989. He is currently a Professor with Shenzhen University. His research interests include intelligent information processing and pattern recognition.

JIHONG PEI received the B.S. degree in electronics engineering from Beihang University in 1989 and the M.S. degree in physical electronics and optoelectronics and the Ph.D. degree in signal and information processing from Xidian University in 1994 and 1998, respectively. He is currently a Professor with Shenzhen University. His research interests include intelligent information processing and pattern recognition.

KELI HU received the B.S. degree in communication engineering from Hangzhou Dianzi University in 2009 and the Ph.D. degree in information and communication engineering from the Shanghai Institute of Microsystem and Information Technology, Chinese Academy of Sciences, in 2014. He is currently a Lecturer with Shaoxing University. His research interests include intelligent information processing, pattern recognition, and computer vision and image processing.

XIAOBIN LI received the B.S. degree in computer science and technology from Northwest Normal University, Lanzhou, China, in 2002, and the M.S. degree in computer science from Jožef Stefan International Postgraduate School, Ljubljana, Slovenia, in 2011, where he is currently pursuing the Ph.D. degree. His research interests include multiple target tracking and software engineering.